Three-degree-of-freedom Parallel Manipulator to Track the Sun for Concentrated Solar Power Systems

ASHITH SHYAM R B and GHOSAL A
Robotics and Design Lab, Department of Mechanical Engineering, Indian Institute of Science, Bangalore, 560012, India

Abstract: In concentrated solar power(CSP) generating stations, incident solar energy is reflected from a large number of mirrors or heliostats to a faraway receiver. In typical CSP installations, the mirror needs to be moved about two axes independently using two actuators in series with the mirror effectively mounted at a single point. A three degree-of-freedom parallel manipulator, namely the 3-RPS parallel manipulator, is proposed to track the sun. The proposed 3-RPS parallel manipulator supports the load of the mirror, structure and wind loading at three points resulting in less deflection, and thus a much larger mirror can be moved with the required tracking accuracy and without increasing the weight of the support structure. The kinematics equations to determine motion of the actuated prismatic joints in the 3-RPS parallel manipulator such that the suns rays are reflected on to a stationary receiver are developed. Using finite element analysis, it is shown that for same sized mirror, wind loading and maximum deflection requirement, the weight of the support structure is between 15% and 60% less with the 3-RPS parallel manipulator when compared to azimuth-elevation or the target-aligned configurations.

Keywords: 3-RPS, Parallel manipulator, Heliostat, Solar tracking

1 Introduction

Research and development of clean energy systems have been gaining in acceptance and use in the recent past. Solar energy being the most abundant, renewable, non-pollutant and available throughout the year has the highest potential from which clean energy can be harvested. The popular methods to harvest solar energy is the use of photo-voltaic cells, parabolic troughs and dishes, central receiver tower system etc. In this paper, the focus is on concentrated solar power (CSP) approach where the suns energy is concentrated at a central receiver tower and then converted to electricity. As pointed out by VANT-HULL [1], one of the advantages of CSP over other solar energy harvesting approaches is higher thermal efficiency and lower operating cost. Additionally, in the CSP approach, thermal energy can be stored using molten salt which enables the production of electricity even when there is no sunlight [2]. HBERLE [3] reported that the thermal energy can also be used to generate process steam for industrial application..

The sun moves in a general East to West direction during the day and in a North-South direction during seasons. To focus the suns energy on to the central receiver, mirrors are used and the mirrors must be moved to accommodate the sun's apparent motion in the sky. The first of these moving mirrors, also called heliostats, were built by TROMBE Felix at Odellio, France in the 1950s [1]. He used these heliostats to direct the sun rays on to a fixed horizontal parabola as parallel beams of light. In modern CSP plants, there exist two well-known methods for moving the heliostats. These are called the azimuth- elevation (Az-El) and target-aligned (T-A) (also called the spinning-elevation) methods with the azimuth-elevation method more widely implemented. In both the above methods, there are two actuators which track the sun and orient the heliostats(see Fig. 1) in such a way that the incident ray from the sun is always reflected onto a fixed central receiver.

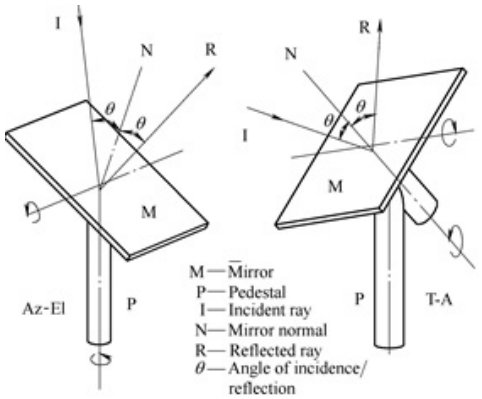

Figure 1: Schematic of the Az-El and T-A configurations

Though simple and economical, the Az-El method of tracking has got numerous disadvantages [1]. In order to overcome the short comings of the Az-El method, RIES, et al [4], and ZAIBEL, et al [5], proposed the use of a target aligned mount. CHEN, et al [6] and WEI, et al [7], derived the formulas for sun tracking for the T-A heliostat. To increase the concentration of incident solar radiation, the mirrors are typically canted–the arrangement of mirrors such that it approximates a paraboloid of revolution. There are different types of canting methods like on-axis, off-axis and parabolic canting. A comprehensive study of these methods has been made by BUCK, et al [8]. Even though canting gives a better concentration ratio, it effectively modifies the focal point and introduces what is called the off-axis aberration as reported by RABL [9].

As shown in Fig. 1, the mirrors are supported by a support frame and a pedestal which is fixed to the ground. The pedestal with the drives for the Az-El and the T-A heliostats are typically placed at the geometrical center of the mirror assembly. Due to this arrangement, the deflection of the support frame and the mirrors due to self-weight and wind load can go beyond the allowable slope error limit of 2-3 mrad [1] at the edges or corner of the mirror structure. In order to tackle this problem, either the support frame has to be made more rigid or smaller sized heliostats have to be used. A larger number of smaller heliostats imply the use

of more actuators and sometimes loss of harvested energy due to blocking of one by another.

Both the azimuth-elevation and the target-aligned arrangement are kinematically in a serial configuration and as in any serial configuration the tracking error is the sum of the errors of the two actuators. To reduce tracking error to less than the required 2 mrad, accurate and expensive gear boxes need to be used to achieve the large gear reduction required to track the motion of sun (approximately radians in 12 h). In this paper, we propose the use of a three-degree-of-freedom parallel manipulator, namely the well-known 3-RPS parallel manipulator. As in any general parallel manipulator, the payload, in this case the mirror and support structure subjected to gravity and wind loading is supported at more than one point. As a result the payload can be much larger and the tracking accuracy will be governed by the largest error in an actuator [10]. In spite of the use of an extra actuator, as compared to the azimuth-elevation and target-aligned method, it is expected that the overall cost of the heliostat per unit area, especially for larger heliostats, will be lower with the 3-RPS parallel manipulator. Google Inc. [11] [12] also developed a novel method for changing the position and orientation of the reflector(mirror). They propose the use of an electric cable drive system which is constantly under tension. They also claim that this method will reduce the power consumption, size and cost of the actuator system.

This paper is organized as follows: In section 2, this paper presents a brief description of the three-degree- of-freedom parallel 3-RPS manipulator, the optics and kinematic equations relating the orientation of the mirror to the motion of the sun in the sky and the motion of the actuated joints required to focus the reflected sun radiation on to a fixed receiver. In section 3, this paper presents the finite element based modeling of the mirror and structure to study the effects of the wind loading and self-weight. In section 4, this paper presents the kinematic and finite element analysis results and demonstrate the advantages of using a parallel manipulator for a heliostat. Finally, in section 5, the conclusions of the work and future directions are presented.

2 Geometry and kinematics of a 3-RPS manipulator

Fig. 2 shows the well-known three-degree-of-freedom 3-RPS parallel manipulator. It consists of a top moving platform which is connected to a fixed base by means of three actuated prismatic(P) joints P_i, i=1, 2, 3. At each of the connection points, S_i, i=1, 2, 3, at the top moving platform, there is a spherical(S) joint and at each of the connection points at the fixed base, R_i, i=1, 2, 3, there is a rotary(R) joint. The axes of the rotary joints are in the plane of the fixed platform. The mirror assembly is fixed to the top moving platform using a support structure which is designed to provide adequate stiffness such that deflections due to wind loads and self-weight are within acceptable limits as mentioned earlier. Even though the mirror assembly can have arbitrary shapes, for the purpose of kinematics only the triangle formed by S_1, S_2 and S_3 need to be considered.

The degrees of freedom of the manipulator can be found out by using the well-known Grbler - Kutzbach equation:

$$dof = (N - J - 1) + F_i,$$

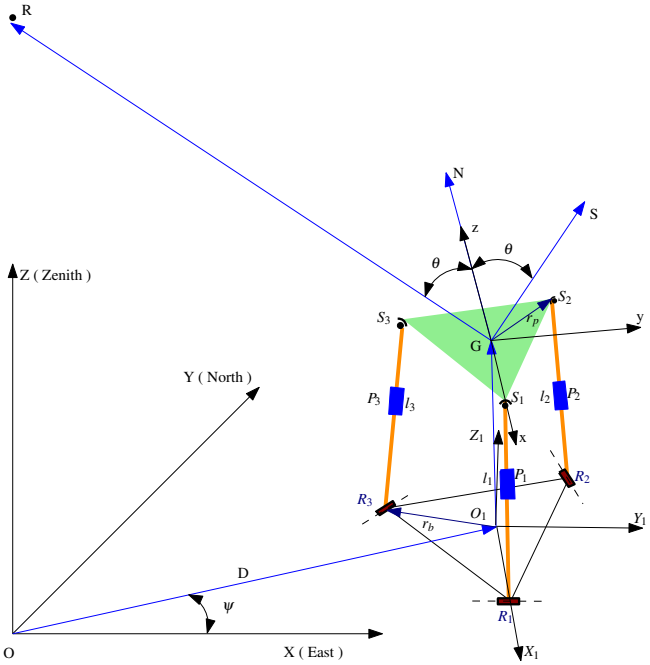

Figure 2: Schematic diagram of a 3-RPS heliostat

where λ is 6 for 3D and 3 for planar motion, N is the number of links including the fixed link, J is the number of joints and F_i is the degrees of freedom of joint i. For the 3-RPS manipulator, N=8, J=9 and F_i =15, and thus dof=3. This implies that three actuators are required to move the top platform [13] [14]. SRIVATSAN, et al [15], has further shown that the three principal motions of the top moving platform are rotation about X and Y axis and a linear motion along the Z axis. For tracking the sun, the rotation capability about the X and Y axes are used. The linear motion along the Z axis can be used to bring the mirror assembly down when high wind speeds are present or for optimization.

Referring to Fig. 2, let O be the origin of the fixed coordinate system, X, Y, Z, and attached to the fixed-base (ground) on the surface of the earth. The axes OX, OY, and OZ point towards local East, local North and the zenith directions, respectively. The foot of the receiver tower and the origin, O, of the fixed coordinate system coincides with each other. The point R denotes the location of the receiver where the incident solar energy is focused by the mirror. Without loss of generality, we assume that the triangle formed by the connection points S_i, i=1, 2, 3 form an equilateral triangle whose circum-radius is rp. The plane of the moving top platform, containing the mirror assembly, is defined by the normal given by the cross product of the vectors and . From the laws of optics, a) the incident ray from the sun and the reflected ray to the receiver make equal angle θ with the normal and b) the incident ray, the normal and the reflected ray lie on a plane

Let l_1, l_2 and l_3 denote the lengths of the prismatic joints at any instant of time. Without loss of generality, we assume that the revolute (R) joints at the fixed base are placed at the corners of an equilateral triangle whose circum-radius is r_b. The centroid of this equilateral triangle is O_1 which

is at a distance, D, from O and at an angle ψ with respect to the OX axis. The co-ordinate system at O_1 with axis $\{X_1, Y_1, Z_1\}$ is described with respect to the fixed coordinate system by a rotation about Z axis and a translation along $\overrightarrow{OO_1}$. The coordinate system at G is denoted with $\{x, y, z\}$ and the vector $\overrightarrow{O_1G}$ is denoted by $[x_c, y_c, z_c]^T$. The homogeneous transformation matrix $[T]$ which relates the coordinate system at O_1 and G can be described by,

$$[T] = \begin{bmatrix} n_1 & o_1 & a_1 & x_c \\ n_2 & o_2 & a_2 & y_c \\ n_3 & o_3 & a_3 & z_c \\ 0 & 0 & 0 & 1 \end{bmatrix}$$

where the column vectors $(n_1, n_2, n_3)^T$, $(o_1, o_2, o_3)^T$ and $(a_1, a_2, a_3)^T$ determine the orientation of the moving platform.

2.1 Kinematics of a 3-RPS heliostat

In the kinematics of a 3-RPS manipulator, there are two well-known problems. In the direct kinematics problem, the prismatic joint variables l_1, l_2 and l_3 are known and the position vector $(x_c, y_c, z_c)^T$ and the orientation of the top platform or T is to be found out. In the inverse kinematics problem, for a given T the prismatic joint variables need to be obtained. For sun tracking, we are primarily interested in the inverse kinematics of the 3-RPS manipulator. The elements of the transformation matrix can be computed from the knowledge of suns direction vector, the location of the central receiver tower and the location of the heliostats in a field. Once the transformation matrix T is found out, the leg lengths of the manipulator can be calculated as a function of time.

The unit vector pointing to the sun is denoted by $\overrightarrow{GS}$ and is obtained by knowing the azimuth and elevation angles (The azimuth and elevation angle of the sun depends on the time of the day and the latitude and longitude of the place on the surface of the Earth. This is available from websites [16] or from programs available in literature). These two angles, as a function of time, completely describe the apparent motion of the sun in the sky. Since the 3-RPS has three degrees of freedom and the tracking of the sun requires only two variables, there are several constraint equations relating the 9 unknowns in the transformation matrix T. As mentioned earlier the rotation about the X and Y axis are used for orienting the top platform and one can choose the vertical motion of the top platform, z_c arbitrarily. To obtain the other constraints we proceed as follows.

As for any transformation matrix, we can write five constraint equations as

$$n_1^2 + n_2^2 + n_3^2 = 1 \quad (1)$$
$$o_1^2 + o_2^2 + o_3^2 = 1 \quad (2)$$
$$n_1a_1 + n_2a_2 + n_3a_3 = 0 \quad (3)$$
$$n_1o_1 + n_2o_2 + n_3o_3 = 0 \quad (4)$$
$$o_1a_1 + o_2a_2 + o_3a_3 = 0 \quad (5)$$

The unit vector from the center of the moving platform to the receiver is given by $\overrightarrow{GR}$. The angle bisector which is also the normal to the platform, $\overrightarrow{GN}$, is given by

$$\overrightarrow{GN} = \frac{\overrightarrow{GS} + \overrightarrow{GR}}{||\overrightarrow{GS} + \overrightarrow{GR}||}$$

The vector $\overrightarrow{GR}$ is a function of x_c, y_c and the assumed value of z_c and since $\overrightarrow{GS}$ is known in terms of azimuth and elevation angles, the normal $\overrightarrow{GN}$ is also a function of the azimuth and elevation angles of the sun and x_c, y_c and the assumed value of z_c. This implies that the direction cosines a_1, a_2 and a_3 of the normal vector $\overrightarrow{GN}$ are functions of five variables.

The 3-RPS configuration introduces additional three constraints [4] given by

$$y_c + n_2r_p = 0 \quad (6)$$
$$n_2 = o_1 \quad (7)$$
$$x_c = \frac{r_p}{2}(n_1 - o_2) \quad (8)$$

where r_p is the distance of the vertices from the centre of the moving platform. Thus there are 8 equations in 8 unknowns, i.e., $\{x_c, y_c, n_1, n_2, n_3, o_1, o_2, o_3\}$. From equations (6) and (7),

$$n_2 = o_1 = \frac{-y_c}{r_p}$$

and from equation (8),

$$o_2 = n_1 - \frac{2x_c}{r_p}$$

Eliminating n_2, o_1 and o_2, we get

$$n_1^2 + (\frac{y_c}{r_p})^2 + n_3^2 = 1 \quad (9)$$
$$(\frac{y_c}{r_p})^2 + (n_1 - \frac{2x_c}{r_p})^2 + o_3^2 = 1 \quad (10)$$
$$n_1a_1 - \frac{y_c}{r_p}a_2 + n_3a_3 = 0 \quad (11)$$
$$-2n_1\frac{y_c}{r} + \frac{2x_cy_c}{r_p^2} + n_3o_3 = 0 \quad (12)$$
$$\frac{-y_c}{r_p}a_1 + (n_1 - \frac{2x_c}{r_p})a_2 + o_3a_3 = 0 \quad (13)$$

Thus we can arrive at 5 equations in 5 unknowns, i.e., $(n_1, n_3, o_3, x_c$ and $y_c)$ which can be further reduced by substitution and using Bezout's method of elimination. Finally we can get two equations in x_c and y_c given in equation (14) and equation (15) below. Equations (14) and (15) are numerically solved for x_c and y_c in MATLAB® using the inbuilt routine *fsolve* [18] for a given a_1, a_2 and a_3. The two equations are as follows:.

$$d_1x_c^2 + e_1x_c + f_1 = 0, \quad (14)$$
$$d_2x_c^2 + e_2x_c + f_2 = 0, \quad (15)$$

where

$$d_1 = -12\frac{{y_c}^2{a_2}^2}{{a_1}^2r^4} - 4\frac{{y_c}^2}{r^4} - 4\frac{{y_c}^2{a_2}^4}{{a_1}^4r^4} + 4\frac{{a_2}^2}{r^2{a_3}^2}$$
$$- 4\frac{{y_c}^2{a_2}^4}{r^4{a_3}^2{a_1}^2} + 4\frac{{a_2}^2}{{a_1}^2r^2} - 8\frac{{a_3}^2{y_c}^2{a_2}^2}{{a_1}^4r^4} - 4\frac{{y_c}^2{a_2}^2}{r^4{a_3}^2}$$
$$- 4\frac{{a_3}^4{y_c}^2}{{a_1}^4r^4} - 8\frac{{a_3}^2{y_c}^2}{{a_1}^2r^4}$$

$$e_1 = -4\frac{a_1{y_c}^3a_2}{r^4{a_3}^2} - 4\frac{{a_2}^5y_c}{{a_1}^3{a_3}^2r^2} + 4\frac{y_c{a_2}^3}{r^2a_1{a_3}^2}$$
$$- 4\frac{{a_3}^2y_ca_2}{{a_1}^3r^2} + 4\frac{{y_c}^3{a_2}^5}{r^4{a_1}^3{a_3}^2} - 8\frac{y_c{a_2}^3}{{a_1}^3r^2} - 4\frac{{y_c}^3a_2}{r^4a_1} + 4\frac{{y_c}^3{a_2}^3}{r^4{a_1}^3}$$

$$f_1 = \frac{{y_c}^2}{{r_p}^2} - 5\frac{{y_c}^4{a_2}^4}{{r_p}^4{a_1}^4} - \frac{{a_2}^2}{{a_1}^2} + \frac{{y_c}^4{a_2}^4}{{r_p}^4{a_1}^2{a_3}^2} + \frac{{a_2}^6{y_c}^2}{{a_1}^4{a_3}^2{r_p}^2} +$$
$$4\frac{{a_3}^4{y_c}^2}{{a_1}^4{r_p}^2} - 4\frac{{a_3}^4{y_c}^4}{{r_p}^4{a_1}^4} + 4\frac{{a_3}^2{y_c}^2}{{a_1}^2{r_p}^2} - 8\frac{{a_3}^2{y_c}^4}{{r_p}^4{a_1}^2} - 5\frac{{y_c}^4}{{r_p}^4} -$$
$$\frac{{a_1}^2{y_c}^4}{{r_p}^4{a_3}^2} - 6\frac{{y_c}^4{a_2}^2}{{r_p}^4{a_1}^2} + 8\frac{{a_3}^2{y_c}^2{a_2}^2}{{a_1}^4{r_p}^2} - 8\frac{{y_c}^4{a_3}^2{a_2}^2}{{r_p}^4{a_1}^4} +$$
$$\frac{{y_c}^4{a_2}^2}{{r_p}^4{a_3}^2} + 5\frac{{y_c}^2{a_2}^4}{{a_1}^4{r_p}^2} - 2\frac{{y_c}^2{a_2}^4}{{r_p}^2{a_1}^2{a_3}^2} +$$
$$2\frac{{y_c}^2{a_2}^2}{{a_1}^2{r_p}^2} + \frac{{y_c}^2{a_2}^2}{{r_p}^2{a_3}^2} - \frac{{y_c}^4{a_2}^6}{{r_p}^4{a_1}^4{a_3}^2}$$

$$d_2 = -4\frac{{a_3}^4{y_c}^2}{{a_1}^4{r_p}^4} - 4\frac{{a_2}^4{y_c}^2}{{a_1}^4{r_p}^4} - 4\frac{{a_2}^4{y_c}^2}{{r_p}^4{a_3}^2{a_1}^2}$$
$$+ 4\frac{{a_2}^4}{{r_p}^2{a_1}^2{a_3}^2} - 8\frac{{a_3}^2{y_c}^2}{{a_1}^2{r_p}^4} + 4\frac{{a_2}^2}{{r_p}^2{a_1}^2} - 8\frac{{a_3}^2{a_2}^2{y_c}^2}{{a_1}^4{r_p}^4}$$
$$- 4\frac{{a_2}^2{y_c}^2}{{r_p}^4{a_3}^2} - 12\frac{{a_2}^2{y_c}^2}{{a_1}^2{r_p}^4} - 4\frac{{y_c}^2}{{r_p}^4}$$

$$e_2 = -4\frac{a_1{y_c}^3a_2}{{r_p}^4{a_3}^2} - 4\frac{{a_2}^5y_c}{{a_1}^3{a_3}^2{r_p}^2} + 4\frac{y_c{a_2}^3}{{r_p}^2a_1{a_3}^2} - 4\frac{{a_3}^2y_ca_2}{{a_1}^3{r_p}^2}$$
$$+ 4\frac{{y_c}^3{a_2}^5}{{r_p}^4{a_1}^3{a_3}^2} - 8\frac{y_c{a_2}^3}{{a_1}^3{r_p}^2} - 4\frac{{y_c}^3a_2}{{r_p}^4a_1} + 4\frac{{y_c}^3{a_2}^3}{{r_p}^4{a_1}^3}$$

$$f_2 = \frac{{y_c}^2}{{r_p}^2} - 5\frac{{y_c}^4{a_2}^4}{{r_p}^4{a_1}^4} - \frac{{a_2}^2}{{a_1}^2} + \frac{{y_c}^4{a_2}^4}{{r_p}^4{a_1}^2{a_3}^2} + \frac{{a_2}^6{y_c}^2}{{a_1}^4{a_3}^2{r_p}^2} +$$
$$4\frac{{a_3}^4{y_c}^2}{{a_1}^4{r_p}^2} - 4\frac{{a_3}^4{y_c}^4}{{r_p}^4{a_1}^4} + 4\frac{{a_3}^2{y_c}^2}{{a_1}^2{r_p}^2} - 8\frac{{a_3}^2{y_c}^4}{{r_p}^4{a_1}^2} - 5\frac{{y_c}^4}{{r_p}^4} -$$
$$\frac{{a_1}^2{y_c}^4}{{r_p}^4{a_3}^2} - 6\frac{{y_c}^4{a_2}^2}{{r_p}^4{a_1}^2} + 8\frac{{a_3}^2{y_c}^2{a_2}^2}{{a_1}^4{r_p}^2} - 8\frac{{y_c}^4{a_3}^2{a_2}^2}{{r_p}^4{a_1}^4} + \frac{{y_c}^4{a_2}^2}{{r_p}^4{a_3}^2}$$
$$+ 5\frac{{y_c}^2{a_2}^4}{{a_1}^4{r_p}^2} - 2\frac{{y_c}^2{a_2}^4}{{r_p}^2{a_1}^2{a_3}^2} + 2\frac{{y_c}^2{a_2}^2}{{a_1}^2{r_p}^2} + \frac{{y_c}^2{a_2}^2}{{r_p}^2{a_3}^2} - \frac{{y_c}^4{a_2}^6}{{r_p}^4{a_1}^4{a_3}^2}$$

As mentioned earlier a_1, a_2 and a_3 are the direction cosines of the vector $\overrightarrow{GN}$ and are dependent on the azimuth and elevation of the sun (or $\overrightarrow{GS}$) and x_c, y_c and the assumed value of z_c. The computed x_c and y_c values along with the arbitrarily chosen value for z_c give the vector and all the other unknowns in the transformation matrix can be obtained.

2.2 Determination of leg lengths

From the geometry of the 3-RPS manipulator, the co-ordinates of the revolute joints with respect to $\{X_1, Y_1, Z_1\}$ are given by $\overrightarrow{O_1R_1} = [r_b, 0, 0]^T$, $\overrightarrow{O_1R_2} = [-\frac{1}{2}r_b, \frac{\sqrt{3}}{2}r_b, 0]^T$ and $\overrightarrow{O_1R_3} = [-\frac{1}{2}r_b, -\frac{\sqrt{3}}{2}r_b, 0]^T$ and the co-ordinates of the spherical joints with respect to $\{x, y, z\}$ are given by $\overrightarrow{GS_1} = [r_p, 0, 0]^T$, $\overrightarrow{GS_2} = [-\frac{1}{2}r_p, \frac{\sqrt{3}}{2}r_p, 0]^T$ and $\overrightarrow{GS_3} = [-\frac{1}{2}r_p, -\frac{\sqrt{3}}{2}r_p, 0]^T$. The position vector of the spherical joints with respect to the co-ordinate system $\{X_1, Y_1, Z_1\}$ is given as

$$\begin{bmatrix} \overrightarrow{O_1S_i} \\ 1 \end{bmatrix} = [T] \begin{bmatrix} \overrightarrow{GS_i} \\ 1 \end{bmatrix}$$

The leg lengths can be found out as shown in reference [13] as

$$l_i = ||\overrightarrow{O_1R_i} - \overrightarrow{O_1S_i}||$$

where $i = 1, 2, 3$ and $||$ represents the norm of the vector.In the next section, we present a finite element method based modeling of the mirror and the support structure to determine deflections due to wind loading and self weight.

3 Finite element modeling of mirror and support structure

The finite element analysis of the mirror and support structure is done in ANSYS® Workbench [19]. The element types used are *SOLID186* and *SOLID187* with three degrees of freedom per node. Program controlled automatic meshing is enabled for the analysis. The mesh size is refined in each iteration until convergence is achieved.

The deformation of the mirror and support structure is found out for its self-weight and for a survival wind speed, v of 22 m/s and an operational wind speed, v of 10 m/s. The guidelines for wind load calculation are given in PETERKA, et al [20] [21]. The structure is kept vertically so that the worst case scenario can be simulated. The factor of safety(FoS) used for the analysis is 2. The uniform wind load(P) on the surface of the mirror is calculated by using the equation

$$P = \frac{1}{2}C_d\rho v^2 FoS$$

where $C_d = 1.18$ is the drag coefficient and ρ is the density of air assumed to be 1.25 kg/m^3 (see Fig. 3). The mirror is assumed to be made of float glass weighing 10 kg/m^2 and we have created models of various sizes – results for 2m $\times$ 2m, 3m $\times$ 3m and 5m $\times$ 5m are presented. We have attempted various configurations of support structures and supporting material, made of low carbon steel, of different cross-section and wall thickness. The CAD model of the support structure and the mirror was made using SolidWorks® [22] and the two were *mated* to obtain a single object and then ported to ANSYS®Workbench for finite element analysis to obtain the stresses and deformation due to the wind and self-weight loading. The goal of

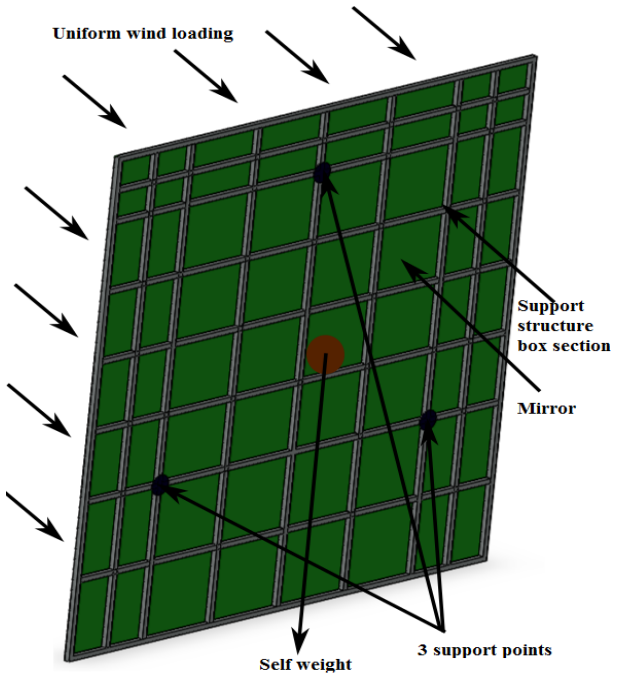

Figure 3: Uniform wind load acting on the mirror

the continuing study is to obtain the lightest possible support structure which satisfies the maximum deformation requirements and thus reduce material cost. We present representative results in the next section.

4 Simulation results

In this section, we present numerical simulation results for the motion of the heliostat to track the sun. We also present finite element analysis to determine deflection of various sized mirrors due to wind load and self-weight. As

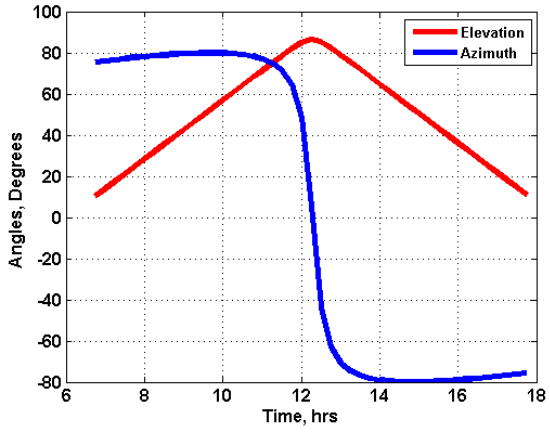

Figure 4: Azimuth and Elevation angles for May 6th 2013 for Bangalore

mentioned earlier the observed motion of the sun in the sky depends on the date and time of the year and also on the

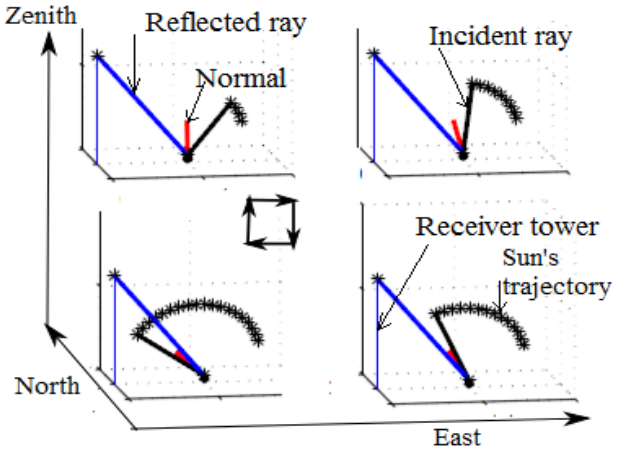

Figure 5: Motion of 3-RPS heliostat with time

latitude and longitude of the location on Earth. We present simulation results for 6th of May 2013 and for Bangalore, India (Latitude 12^0 58′ 13" N and Longitude 77^0 33′ 37" E). The Azimuth and Elevation angles of the sun for the same day and for the same place is shown in Fig. 4. The motion of the 3-RPS based heliostat for different instants of time is simulated in MATLAB® and is shown in Fig.5.

For r_p equal to 0.9 m and r_b equal to 1m, the leg lengths (actuated joints) of the 3-RPS based heliostat are computed and is plotted for summer solstice (June 21) and winter solstice (December 21) and is shown in Figs. 6 and 7. The central receiver tower for the above calculations is kept at (0, 0, 65)m with respect to the fixed co-ordinate system. It can be seen that the leg lengths change during the day and the plot of the leg length variation also changes with the season. Although not shown, the change in the leg lengths also depend on the location of the heliostat in the solar field. Such simulations of the motion of the heliostat can be used to choose the stroke of the linear actuator which will change the leg lengths.

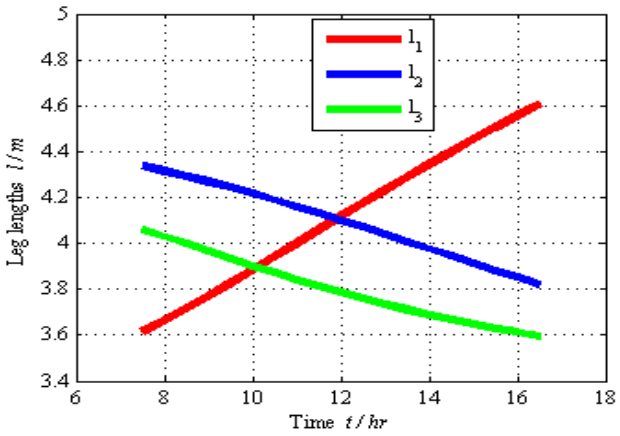

Figure 6: Leg length variation for summer solstice

Figs. 8 - 10 show the finite element analysis results for three heliostats. Tables 1 and 2 show the maximum defor-

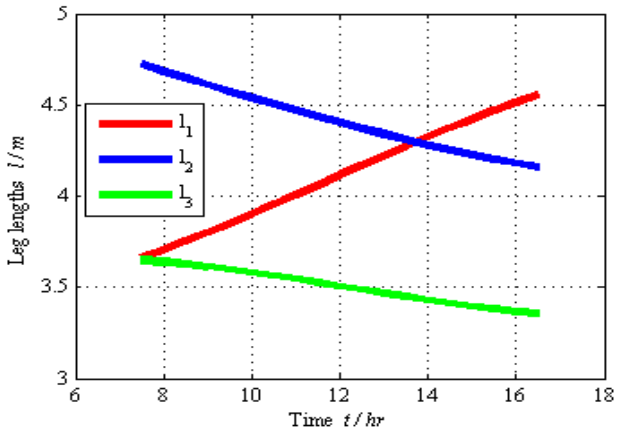

Figure 7: Leg length variation for winter solstice

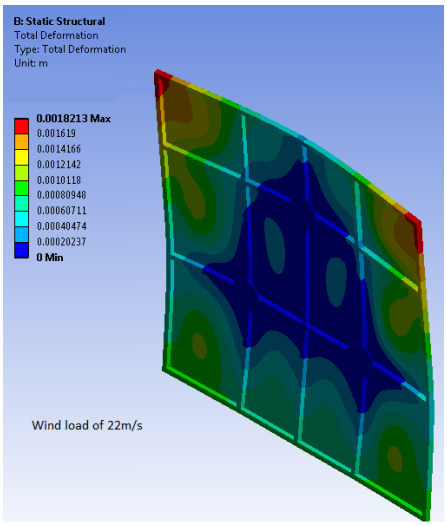

Figure 8: Deformation of a 2m x 2m mirror

mation and the weight of the support structure required in each of the three heliostats for two different wind speed of 10 m/s and 22 m/s – the heliostat is designed to function for wind speeds up to 10 m/s and must be able to withstand wind speeds and gusts up to 22 m/s.

The details of the sections used for the finite element analysis are as follows: :

1. Wind speed of 22 m/s
    - For 2 m $\times$ 2 m the results are for square box section of size 30 mm and wall thickness of 2 mm.
    - For 3 m $\times$ 3 m the results are for square box section of size 50 mm and wall thickness of 2 mm.
    - For 5 m $\times$ 5 m the results are for square box section of size 70 mm and wall thickness of 3 mm.
2. Wind speed of 10 m/s

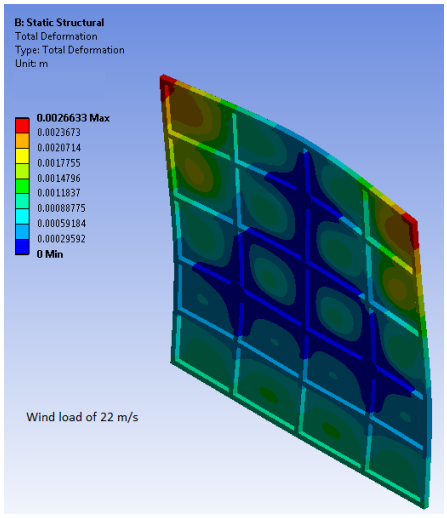

Figure 9: Deformation of a 3m x 3m mirror

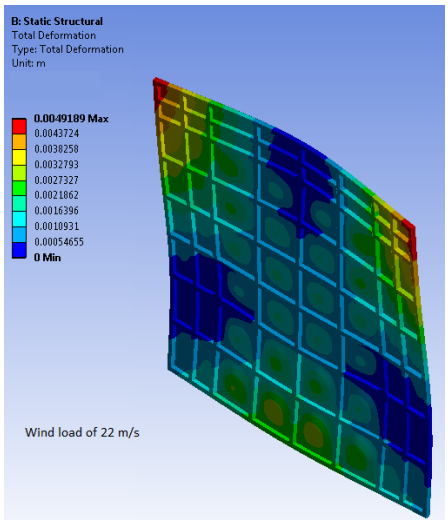

Figure 10: Deformation of a 5m x 5m mirror

- For 2 m $\times$ 2 m the results are for square box section of size 20 mm and wall thickness of 2 mm.
- For 3 m $\times$ 3 m the results are for square box section of size 30 mm and wall thickness of 2 mm.
- For 5 m $\times$ 5 m the results are for square box section of size 50 mm and wall thickness of 2.5 mm.

The maximum stress values are not shown as they are very small and the maximum deformation is of interest. For comparison, we also made finite element models of each of the three heliostat with single point support thus simulating the currently used Azimuth-Elevation and Target-Aligned system of actuation. From the figures and tables, it can be seen that the slope error is less than 2 mrad everywhere.

For meeting the 2 mrad maximum deflection criterion, it can be seen that the weight of the support structure is much

Table 1: Comparison of weight and deflection for 3-RPS and Az-El heliostat (v=10 m/s)

Wind loading of 10 m/s				
Mirror size L x B / (m x m)	**Support structure weight W/ kg**		**Deflection δ / mm**	
	3-RPS	**Az-El**	**3-RPS**	**Az-El**
2 x 2	15	20.94	1.93	1.87
3 x 3	45	53.53	2.45	2.65
5 x 5	198	356.97	4.90	4.74

Table 2: Comparison of weight and deflection for 3-RPS and Az-El heliostat (v=22 m/s)

Wind loading of 22 m/s				
Mirror size L x B / (m x m)	**Support structure weight W/ kg**		**Deflection δ / mm**	
	3-RPS	**Az-El**	**3-RPS**	**Az-El**
2 x 2	30	35.50	1.82	1.93
3 x 3	93	181.20	2.66	2.87
5 x 5	535	1332.55	4.92	4.74

less with the three point support available when the parallel 3-RPS manipulator is used. The reduction in weight varies from 15% to 60% when compared with the Az-El configuration with more reduction in weight for the larger 5m $\times$ 5m configuration.

5 Conclusions and challenges ahead

1. The kinematic equations of the parallel 3-RPS manipulator were obtained. It is shown that the 3-RPS manipulator can be used for tracking the sun in concentrated solar power systems.

2. Based on a finite element analysis of the 3-RPS based heliostat it is shown that the support structure is 15% to 60%less as compared to the existing Azimuth-Elevation or Target-Aligned configurations used in current heliostats. Alternately, for a given weight of the support structure and pointing accuracy requirement, the 3-RPS heliostat can carry a larger mirror.

3. Due to the lower weight, the 3-RPS based heliostat is expected to be less expensive. The 3-RPS based heliostat is also expected to be more accurate due to its parallel structure.

The work is continuing. One of the major challenges is to find a good way to fix the mirror(s) to the support structure and to obtain an optimum value for the radius of the circumscribing circle rp. A change in rp value not only changes the stroke of the linear actuators but also the maximum deformation at the edges of the mirror. If the value of rp is large, the prismatic joints have to be moved more to get the required orientation of the moving platform and if it is less, then the deformation at the edges will be larger. Another issue is to make use of the third degree of freedom available in the 3-RPS manipulator, namely the translational motion along the vertical direction, in interesting ways or optimizing an useful objective function

Acknowledgment

This research is based upon work supported in part by the Solar Energy Research Institute for India and the U.S. (SERIIUS) funded jointly by the U.S. Department of Energy subcontract DE AC36-08G028308 (Office of Science, Office of Basic Energy Sciences, and Energy Efficiency and Renewable Energy, Solar Energy Technology Program, with support from the Office of International Affairs) and the Government of India subcontract IUSSTF/JCERDCSERIIUS /2012 dated 22nd Nov. 2012.

The authors would also like to thank Mohit Acharya who helped in obtaining results relating to maximum deflection of the mirror assembly for the Azimuth-Elevation configuration.

References

1. VANT-HULL L L. Chapter 8 Central tower concentrating solar power(CSP) systems[M/OL]//Keith Lovegrove and Wes Stein, eds. Concentrating solar power technology. Philadelphia: Woodhead Publishing, 2012: 240283. http://www.sciencedirect.com/science/article/pii/ B978184569769350008X.
2. KOLB G J, SCOTT A J, MATTHEW W D, et al. Heliostat cost reduction study[M/OL]. New Mexico: Sandia National Laboratories, 2007. http://prod.sandia.gov/techlib/access-control.cgi/2007/073293. pdf.
3. HBERLE A. Chapter 19 Concentrating solar technologies for industrial process heat and cooling[M/OL]// Keith Lovegrove and Wes Stein, eds. Concentrating solar power technology. Philadelphia: Woodhead Publishing, 2012: 602619.http://www.sciencedirect.com/science/ article/pii/B9781845697693500194.
4. RIES H, SCHUBNELL M. The optics of a two-stage solar furnace[J]. Solar Energy Materials, 1990, 21(23): 213217.
5. ZAIBEL R, DAGAN E, KARNI J, et al. An astigmatic corrected target-aligned heliostat for high concentration[J]. Solar Energy Materials and Solar Cells, 1995, 37(2): 191202.
6. CHEN Y T, CHONG K K, BLIGH T P, et al. Non imaging focusing heliostat[J]. Solar Energy, 2001, 71(3): 155164.
7. WEI Xiudong, LU Zhenwu, YU Weixing, et al. Tracking and ray tracing equations for the target-aligned heliostat for solar tower power plants[J]. Renewable Energy, 2011, 36(10): 26872693.
8. BUCK R, TEUFEL E. Comparison and optimization of heliostat canting methods[J]. ASME Journal of Solar Energy Engineering, 2009, 131(1): 011001 (8 pages).
9. RABL A. Active solar collectors and their applications[M]. New York: Oxford University Press, 1985.

10. MERLET J P. Parallel robots[M]. 2nd ed. Dordrecht: Springer, 2006.
11. HOpS: The heliostat optical simulation[OL]. Mountain View, CA: Google Inc., 2012. http://hops.googlecode.com/svn/trunk/ doc/hops. html.
12. RE¡C: Heliostat cable actuation system design[OL]. Mountain View, CA: Google Inc. 2012. http://www.google.org/pdfs/google˙ heliostat˙ cable˙actuation.pdf.
13. GHOSAL A. Robotics fundamental concepts and analysis[M]. New Delhi: Oxford University Press, 2006.
14. LEE K M, SHAH D. Kinematic analysis of three degrees of freedom in-parallel actuated manipulator[J]. IEEE Journal of Robotics and Automation, 1988, 4(2): 354360.
15. SRIVATSAN R A, BANDYOPADHYAY S, GHOSAL A. Analysis of the degrees-of-freedom of spatial parallel manipulators in regular and singular configurations[J]. Mechanism and Machine Theory, 2013, 69: 127141.
16. BOWDEN S, HONSBERG C. Pveducation.org[OL]. Tempe, AZ: Solar Power Laboratory, Arizona State University Research Park, 2014.http://pveducation.org/pvcdrom/properties-of-sunlight/azimuth-angle.
17. SALMON G. Lessons introductory to modern higher algebra[M]. 5th ed. Chelsea Publishing Co., 1986.
18. MATLAB version 7.12.0(R2011a)[CP]. The MathWorks Inc., Natick, MA, 2012.
19. ANSYS Workbench version 14.0[CP]. Ansys Inc., Canonsburg, PA, 2011.
20. PETERKA J A, HOSOYA N, BIENKIEWICZ B, et al. Wind load reduction for heliostats[M/OL]. Colorado: Solar Energy Research Institute, 1986: SERI/STR-256-2859, DE86010703. http://www.nrel. gov/ docs/ legosti/old/2859.pdf
21. PETERKA J A, TAN Z, BIENKIEWICZ B, et al. Wind loads on heliostats and parabolic dish collectors[M/OL]. Colorado: Solar Energy Research Institute, 1988: SERI/STR-253-3431, DE89000852. http://www.nrel.gov/docs/legosti/old/3431.pdf.
22. SolidWorks 2013[CP]. Dassault Systems, Waltham, MA, 2013.

Biographical notes

ASHITH SHYAM R B was born in 1984 and is currently a research scholar at Indian Institute of Science, Bangalore, India. He received his master degree from Indian Institute of Science in 2011. His research interests are in the field of dynamics, optimization, vibrations and robotics. E-mail: *shyamashi@gmail.com*

GHOSAL A was born in 1959 and is currently a professor at Department of Mechanical Engineering, Indian Institute of Science Bangalore, India. He received his PhD degree from Stanford University in 1986. His research interests are in the areas of kinematics, dynamics, control and design of robots and other computer controlled mechanical systems. E-mail: *asitava@mecheng.iisc.ernet.in*